Miscibility and exchange chemical potential of ring polymers in symmetric ring–ring blends

Journal:	*Soft Matter*
Manuscript ID	SM-ART-01-2023-000108.R2
Article Type:	Paper
Date Submitted by the Author:	27-Apr-2023
Complete List of Authors:	Ohkuma, Takahiro; Bridgestone Corporation, Digital Engineering Division Hagita, Katsumi; National Defense Academy, Applied Physics Murashima, Takahiro; Tohoku University, Department of Physics Deguchi, Tetsuo; Ochanomizu University, Department of Physics

Journal Name

Miscibility and exchange chemical potential of ring polymers in symmetric ring–ring blends

Takahiro Ohkuma[a*], Katsumi Hagita[b], Takahiro Murashima[c], and Tetsuo Deguchi[d]

Generally, differences of polymer topologies may affect polymer miscibility even with the same repeated units. In this study, the topological effect of ring polymers on miscibility was investigated by comparing symmetric ring–ring and linear–linear polymer blends. To elucidate the topological effect of ring polymers on mixing free energy, the exchange chemical potential of binary blends was numerically evaluated as a function of composition ϕ by performing semi-grand canonical Monte Carlo and molecular dynamics simulations of a bead–spring model. For ring–ring blends, an effective miscibility parameter was evaluated by comparing the exchange chemical potential with that of the Flory–Huggins model for linear–linear polymer blends. It was confirmed that in the mixed states satisfying $\chi N > 0$, ring–ring blends are more miscible and stable than the linear–linear blends with the same molecular weight. Furthermore, we investigated finite molecular weight dependence on the miscibility parameter, which reflected the statistical probability of interchain interactions in the blends. The simulation results revealed that the molecular weight dependence on the miscibility parameter was smaller in ring–ring blends. The effect of the ring polymers on miscibility was verified to be consistent with the change in the interchain radial distribution function. In ring–ring blends, it was indicated that the topology affected miscibility by reducing the effect of the direct interaction between the components of the blends.

1 Introduction

Ring polymers are a typical class of polymers that do not possess terminal ends[1–4]. The simplest architecture of ring polymers is a single loop without concatenation and knotting. The concatenations and knots of ring polymers do not spontaneously change their topology unless chain-opening or closing chemical reactions occur such as in systems like type II DNA topoisomerases[5–7]. The prohibition of spontaneous concatenations entropically imposes a repulsive effect between the rings[8–14]. Swelling effects of ring polymers in dilute solutions can also result from the constraints of knotting topology.[11,15–18] In this study, we focus on nonconcatenated and unknotted rings in melts, unless otherwise specified. Owing to topological constraints, the chain statistics in the melts may be significantly different from the Gaussian chain statistics of ideal linear chains[3,17,19–24]. For instance, the Flory exponent, ν, of the gyration radii which is $1/2$ in the Gaussian chain, ap-

parently presents a crossover from $1/2$ to $1/3$ with respect to the molecular weight of the ring polymer melts. The crossover can be verified based on several computer simulations as elucidated in the forementioned work[23]. The exponent is demonstrated to be approximately 0.5 for relatively small molecular weights compared with the entanglement molecular weight. Conversely, $\nu \approx 1/3$ is expected in cases wherein the molecular weight is over 10 times larger than the entanglement molecular weight. $\nu \approx 0.4$ is observed to be intermediate. Therefore, ring polymers demonstrate considerable potential for modifying macroscopic properties that are affected by chain conformations and topology.

The rheological properties of ring polymer melts and solutions are the first examples that reflect the effect of ring topology[23,25–31]. In the configurations of a blend of linear and ring polymers, linear chains penetrate the rings, resulting in a long time relaxation mode based on constraint and release dynamics[29,32]. Threading events between two-ring polymers have also been reported in a previous simulation study[33,34]. These events contribute to the rheological properties of the material[35,36]. The mechanical properties of polymer networks composed of or containing ring polymers have also been studied using simulations[31,37,38].

In addition to the rheological and mechanical properties, the phase diagrams of polymer blends and block copolymer melts

[a] Digital engineering division, Bridgestone corporation, Kodaira, 187-8531, Japan
[b] Department of Applied Physics, National Defense Academy, 1-10-20, Hashirimizu, Yokosuka, 239-8686, Japan
[c] Department of Physics, Tohoku University, 6-3, Aramaki-aza-Aoba, Aoba-ku, Sendai, 980-8578, Japan
[d] Department of Physics, Faculty of Core Research, Ochanomizu University, 2-1-1 Ohtsuka, Bunkyo-ku, Tokyo 112-8610, Japan
* takahiro.ohkuma@bridgestone.com

are expected to be affected by ring topology[13,39–48]. When ring polymers are used as additives to alter material properties, miscibility is an important factor for their applicability. In studies focusing on phase behavior within the framework of the random phase approximation[49], scattering functions derived from the assumption of Gaussian statistics for ring polymers have often been used[40,41] while ignoring topological constraints. Monte Carlo simulations can be used for ring polymer blends to consider topological constraints. Using a lattice model, block copolymer rings have been reported to undergo microphase separation at a lower transition temperature than that of the block copolymer melt of linear chains[43]. It was also reported in the review[42] that the critical temperature of macroscopic phase separation in a symmetric ring–ring blend was lower than that of the corresponding linear–linear blend as determined by the Monte Carlo exchange method.

Khokhlov and Nechaev proposed a free energy model[39] that included the topological effect of ring polymer for ring–linear blends based on the standard Flory–Huggins model for linear polymers[50]. They introduced the effect of crumpled conformations of rings in the free energy and discussed the dilution effect by linear polymers. The theory predicted that ring–linear blends exbihited a compatibility enhancement in comparison with the corresponding linear–linear blends. Sakaue and Nakajima introduced the concept of the topological volume of ring polymers for ring–ring, ring–linear, and linear–linear polymer blends[13,44]. For the free energy, the translational entropy is decreased by the decrease of the free volume and a penalty for the conformational collapse of ring polymers were considered. Based on a scaling argument in the Flory–Huggins model, the authors produced phase diagrams of the macroscopic phase separation. In the phase diagrams, the critical temperature of ring–ring and ring–linear blends was predicted to be higher and lower, respectively, than that of the linear–linear blend.

Experimentally, neutron scattering analyses for different blends of poly(4-trimethylsilylstyrene) (h-PT) and deuterated polyisoprene (d-PI) have revealed that although the ring–ring blend is less miscible than the linear–linear and linear–ring blends, the critical temperatures of the linear–linear and linear–ring blends are similar[45]. Thus, the theory and experiment are not qualitatively mutually exclusive; however, a quantitative comparison is not trivial. In particular, molecular weights sufficiently larger than the entanglement molecular weight are assumed in the theoretical model based on the scaling argument. A study for finite molecular weight effects is practically needed because a precision polymerization of ring polymers with large molecular weights is not easy. Furthermore, numerical studies to verify the validitity in the phenomenological models are required to invetigate the effect of molecular weights of ring polymers.

Very recently, a simulation study for ring–linear blends with molecular weights around the entanglement molecular weight has also been reported[48]. In the foregoing study, the miscibility of symmetric ring–ring blends was also investigated using semi-grand canonical Monte Carlo (SGMC) simulations, and it was verified that the ring–ring blends are more compatible than the corresponding symmetric linear–linear blends. This result is consistent with that of a previous study on the critical temperature

for ring–ring blends[42]. As the Monte Carlo exchange method is inefficient for asymmetric blends, ring–linear blends were equilibrated by brute-force simulations of a bead–spring model with a three-body bend potential. The foregoing study focused on the miscibility parameter χ in the relationship of scattering functions obtained by the random phase approximation[49]. In the Flory-Huggins model for linear–linear polymer blends, the miscibility parameter is introduced to represent the contribution of the interaction energy between polymer beads. The probability of interaction between the beads is assumed to be propotional to the product of their volume fractions. For linear–linear blends, the difference of the conformational entropy of the chains are neglegible between mixed states and single component melts. On the other hand, the conformational entropy of ring polymers can be different by the archtecture of the surrounding polymers. It was demonstrated that the miscibility parameter which included the entropic contributions of ring polymers can be evaluated from the formula of the random phase approximation. For the ring–linear blends, it was found that an effective miscibility parameter χ was decreased and could be negative. With increasing the chain stiffness, χ becomes more negative because of an entropic stability through the penetration of linear chains into ring polymers.

In this study, symmetric blends of noncocatenated ring polymers with molecular weights near the entanglement molecular weight were investigated by using molecular dynamics (MD) and SGMC simulations. As mentioned above, it has been already reported in the preceding works[42,48] that the critical temperature of symmetric ring–ring blends is lower than that of the corresponding linear–linear blends. Sakaue and Nakajima model does not predict the phase behovior obtained by the simulations for symmetric ring–ring blends. The model needs to phenomenologically take account for further topological effects of ring polymers. Herein, we extended the investigation to the exchange chemical potential μ_{exc} as a function of composition ϕ and investigated the molecular weight dependence. The molecular weight dependence of the miscibility parameter corresponds to the one-loop correction of the composition fluctuation for the interaction energy around the Flory-Huggins mean-field free energy[51–54]. For linear–linear blends, the correction term is of the order of $N^{-1/2}$, where N is the number of segments in a chain, and the prefactor is a universal factor reflecting local configurations based on the chain statistics[52]. Other calibration models to describe the dependence of the molecular weight on the miscibility parameter χ has been evaluated using simulations and experiments[54]. Our aim was to numerically obtain an approximate function $\mu_{\mathrm{exc}}(\phi)$ and verify the topological effect on miscibility resulting from ring configurations in blends with changing molecular weights. The effect of a finite molecular weight on miscibility was compared with the radial distribution functions as a measure of chain configurations. The choice was made to restrict the systems to symmetric blends as these enable efficient executions of Monte Carlo steps during the numerical evaluations. In symmetric blends, all model parameters, except the inter-component interaction strength are identical for both polymer types. For this research, we adopted a flexible bead–spring model[55], as widely used in computational studies of coarse-grained polymers and in previous studies of sym-

metric blends of linear bead–spring polymers[56,57]. The same MD and SGMC calculations were also performed in the study[48] for a bead–spring model with stiffness.

The remainder of this paper is organized as follows. In Section 2, we describe the models and simulations used in this study. The results of SGMC and MD simulations are presented in Section 3, where χN is evaluated for symmertic ring–ring and linear–linear blends using the relationship between μ_{exc} and ϕ. Following this, adopting the first order perturbation approach described in Section 4.1, we demonstrate that the effect of ring polymers on miscibility can be approximately evaluated based on the inter-molecular radial distribution functions. Following this, in Section 4.2, we compare our results with available theoretical and experimental results, before summarizing our findings in Section 5.

2 Methods

In this study, symmetric blend systems, wherein two types of polymers, A and B, were assumed to be chemically identical, were modeled. Only the interaction parameter between A and B was varied in order to determine its effect on the miscibility of the blends. In addtion to the ring–ring symmetric blend systems, symmetric blends consisting of two types of linear polymers were also studied; that is, symmetric linear–linear blends. The polymer chains were modeled using a standard bead-spring chain[55]. The non-bonded interaction between the beads are described by the Weeks–Chandler–Andersen (WCA) potential:

$$V_{s,s'}(r) = \begin{cases} 4\varepsilon_{s,s'}\left[\left(\frac{\sigma}{r}\right)^{12} - \left(\frac{\sigma}{r}\right)^{6} + \frac{1}{4}\right] & (r < r_{\text{cut}}) \\ 0 & (\text{otherwise}) \end{cases} \quad (1)$$

where s and s' represent bead types A and B, respectively, and $r_{\text{cut}} = 2^{1/6}\sigma$. This WCA potential acts on all non-adjacent pairs of beads in the systems. Adjacent beads are bonded by the finitely extensible nonlinear elastic (FENE) potential described as follows:

$$V_{\text{FENE}}(r) = -\frac{1}{2}K\ln\left[1 - \left(\frac{r}{R_0}\right)^2\right] + V_{s,s}(r) \quad (2)$$

where $K = 30\varepsilon_0$ and $R_0 = 1.5\sigma$; here the energy unit is represented by ε_0, and the length unit is represented by σ. It is assumed that $\varepsilon_{\text{AA}} = \varepsilon_{\text{BB}} = \varepsilon_0$ in the symmetric blends. The mass, m, of the beads and the bead size, σ, are also treated as identical for A and B. The number of beads in the ring and linear polymers is denoted by N. The number of beads of the entanglement molecular weight, N_e, is approximately 87 for the linear polymer melts of the bead–spring model[58].

N is varied as $25, 40, 50, 100, 200,$ and 400. The total number of beads equals 50000 for systems with $N = 25, 50, 100,$ and 200, and 80000 for systems with $N = 40$ and 400. The number density of the beads and the temperature of the systems were fixed as $\rho = 0.85\sigma^{-3}$ and $T = \varepsilon_0/k_B$, respectively, where k_B is the Boltzmann constant. We use $m = 1$, $\sigma = 1$, and $\varepsilon_0 = 1$ as the units of mass, length, and energy, respectively. The time unit is $\tau = \sqrt{m\sigma^2/\varepsilon_0}$.

To avoid concatenated and knotted rings in the simulations, we first generated a single ring polymer with a perfect circle shape; the rings were then aligned in a dilute simulation box without
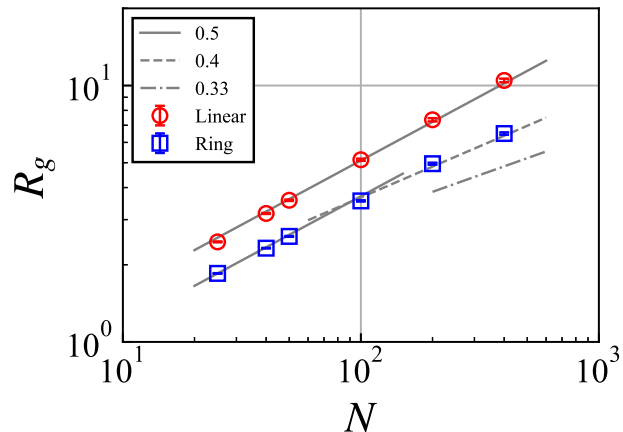

Fig. 1 Gyration radii of the linear and ring polymers at $\varepsilon_{\text{AB}} = \varepsilon_0$ in the melts plotted against the number of beads in a chain N. The solid, dashed, and dot-dashed lines correspond to the exponent $\nu = 0.5$, 0.4, and 0.33 respectively.

concatenations. Following this, the systems were gradually compressed using an *NPT* simulation until the target number density of beads was reached. After compression, the systems were equilibrated by an *NVT* simulation of over $2 \times 10^6 \tau$. Up to this step, the two types of polymers were identical: $\varepsilon_{\text{AB}} = \varepsilon_0$. The gyration radii obtained from the simulations are shown in Fig. 1. As $N_e \approx 87$, it was confirmed that the Flory exponent ν was approximately 0.5 for $N < N_e$ and slightly less than 0.5 for $N_e < N < 10N_e$. The exponent $\nu = 0.5, 0.4$ and 0.33 have been presented in Fig. 1 as references. Once the equilibrium state was obtained, half of the chains were randomly selected and assigned as the bead type A, whereas the other half were assigned as type B. As the bead density is fixed, the systems are expected to undergo a macroscopic phase separation for a sufficiently large $\Delta\varepsilon_{\text{AB}}$ where $\Delta\varepsilon_{\text{AB}} = \varepsilon_{\text{AB}} - \varepsilon_0$ to decrease the interaction energy of the beads. The interaction strength ε_{AB} was varied over ranges in which the linear blend system was reported to be miscible[56,57]: from $\Delta\varepsilon_{\text{AB}}N = -3$ to 3, except for the case where $N = 25$, which was varied over the range -2.5 to 2.5. After the change in ε_{AB}, the systems were again equilibrated by an extended *NVT* simulation, where the mean square displacements of the beads were exceeded 10 times the squared gyration radius of the polymers. (See Supplementary Material)

For symmetric linear–linear blends, we prepared a set of systems in which the number of beads in a chain and the total number of beads were the same as in the symmetric ring–ring blends. Initially, the linear chains were randomly generated in a dilute box. The equilibrium blend states of several ε_{AB} conditions were then obtained by the same procedure as that described for the ring–ring blends. The equilibration procedure of the ring–ring and linear–linear blends was performed using MD simulations with Langevin dynamics using LAMMPS(5May20)[59].

To evaluate the relationship between the exchange chemical potential and the composition, an SGMC simulation was performed in which the bead type A or B in a polymer was exchanged

with the other type according to the Metropolis criterion, as in the previous stduies [56,57,60,61]. The detailed process is as follows: First, one polymer was randomly selected as the candidate for exchange. The energy change caused by the exchange was calculated as $\Delta H = \Delta E \pm \mu_{\mathrm{exc}}$ where ΔE is the energy change of the non-bonded interactions and μ_{exc} is the exchange chemical potential of the polymers. The sign of μ_{exe} is negative when the bead type changes from A to B, and positive when it changes from B to A. The exchange is accepted according to the probability $\min\{1, e^{-\Delta H/k_{\mathrm{B}}T}\}$. Once this has occurred, the bead type changed (i.e., from A to B or vice versa). Therefore, the total number of polymers is preserved, and only the composition was varies. After these exchange attempts, a short MD simulation was performed to relax the polymer configuration of the systems.

The equilibrium composition of A under the condition of μ_{exc} was obtained through alternate SGMC and MD simulations, of which we performed 400 iterations for both the ring–ring and linear–linear blends, according to the methods set out in the previous study [56,57]. The composition ϕ was defined as the ratio of the number of A polymers to the total number of polymers in the blend systems. Futher, $\mu_{\mathrm{exc}}/k_{\mathrm{B}}T$ values of $0.1, 0.2, 0.4, 0.8, 1.6$, and 2.0 were used. In each SGMC process, the number of Monte Carlo attempts was set to half the number of polymers in the system, whereas for each MD process, a 1500τ simulation was performed. Although each MD simulation was shorter than the total relaxation time of the blend systems, it was assumed that the conformations were not significantly different among different compositions when the two components were miscible. The relationship between μ_{exc} and ϕ was therefore evaluated from the combined SGMC/MD simulations. In this study, situations in which the density of one component was too small to be considered as a dilute solution were not explored. All product runs of SGMC/MD simulations were performed using ESPResSo++ [62,63].

To evaluate the miscibility, we focused on the relationship between the exchange chemical potential and the equilibrium composition obtained from the standard Flory–Huggins model for linear–linear polymer blends [50]. The miscibility parameter χ is introdued as a phenomenological parameter and can be determined by fitting experimental or simulation data to the relationship. In practice, the composition dependence of χ is often considered to reproduce complex behaviors such as the phase diagrams of real polymers [64,65] and the volume transition of neutral gels [66]. For ring polymers, additional composition dependence to the standard Flory–Huggins free energy is often considered as in the literatures [13,39,44]. The composition dependence can be verified by evaluating the relationship between the exchange chemical potential and the composition through SGMC simulations. For symmetric linear–linear blends of the bead-spring models, χ can be considered independent of the composition as studied in the literatures [48,56,57]. For symmetric ring–ring and linear–linear blends, we applied the same formula to evaluate χ as an effective miscibility parameter represented as

$$\mu_{\mathrm{exc}}^{(\mathrm{L,R})} = \ln \frac{\phi}{1-\phi} - (\chi N)^{(\mathrm{L,R})} (2\phi - 1) \qquad (3)$$

where the superscript (L) and (R) represent the linear–linear

blends and the ring–ring blends, respectively. We evaluated χN instead of χ by fitting the simulation data to Eq. 3 because χN is scale invariant of coarse-grainned models.

As the exchange chemical potential can be described as $\mu_{\mathrm{exc}} = N(\partial f/\partial \phi)$ where f is the free energy density and the mixed state becomes unstable when $\partial \mu_{\mathrm{exc}}/\partial \phi < 0$, the critical point of phase separation can be obtained by $\partial \mu_{\mathrm{exc}}/\partial \phi = 0$ at $\phi = 0.5$. Therefore, it is possible to evaluate the effect of ring topology on miscibility and compare it with that of $\mu_{\mathrm{exc}}^{(\mathrm{L})}$ and $\mu_{\mathrm{exc}}^{(\mathrm{R})}$.

3 Results

3.1 Relationship between the exchange chemical potential and composition

The equilibrium value of the composition ϕ under the value of μ_{exc} was obtained through SGMC/MD simulations in the symmetric ring–ring and linear–linear blends. The results of the SGMC/MD simulations for the linear–linear and ring–ring blends of $N = 50$ are shown as examples in Figs. 2 a) and b). The value of $\ln\left(\frac{\phi}{1-\phi}\right) - \mu_{\mathrm{exc}}$ is plotted against ϕ so that the gradient represents $2(\chi N)^{(\mathrm{L,R})}$. As shown in Figs. 2 a) and b), linear regression represents the composition dependence well. It indicates that $(\chi N)^{(\mathrm{L,R})}$ can be approximated as composition indepedent parameters. This approximation implies that $\Delta\mu_{\mathrm{ring}} = \mu_{\mathrm{exc}}^{(\mathrm{R})} - \mu_{\mathrm{exc}}^{(\mathrm{L})}$ is proportional to $2\phi - 1$ as verified from Fig. 2 c). Using linear regression, $(\chi N)^{(\mathrm{L,R})}$ can be determined from the slope coefficients as shown in Figs. 3 a) and b) with respect to $\varepsilon_{\mathrm{AB}}$. The interaction strength dependence on $(\chi N)^{(\mathrm{L})}$ is consistent with previously reported results [57] although $\Delta\varepsilon_{\mathrm{AB}}N$.

The relationship between $(\chi N)^{(\mathrm{L})}$ and $(\chi N)^{(\mathrm{R})}$ is summrized in Fig. 3 c) where the miscibility paramters are plotted with respect to the same condition of $\varepsilon_{\mathrm{AB}}$ and N. On increasing the bead interaction difference $|\Delta\varepsilon_{\mathrm{AB}}|$, $|\chi N|$ increases, but the effect of $|\Delta\varepsilon_{\mathrm{AB}}|$ in the ring–ring blends is smaller than that in the corresponding linear–linear blends. Consequently, the ring topology makes the blend slightly more compatible than the linear–linear blend in cases where $\chi N > 0$.

3.2 Finite molecular weight effect

Figure 3 c) presents the relationship between $(\chi N)^{(\mathrm{R})}$ and $(\chi N)^{(\mathrm{L})}$ where the data points are plotted for the same $\varepsilon_{\mathrm{AB}}$ and N. Moreover, the correction for the ring topology effect on miscibility depends weakly on the molecular weight N. To investigate the effect of the finite chain length, we adopted the Flory number n_{F} defined as

$$n_{\mathrm{F}} = \frac{\rho}{N} R_g^3 \qquad (4)$$

where ρ is the bead number density and R_g is the gyration radius of the polymers [50]. The Flory number represents the number of chains in a typical volume characterized by one polymer. The mean-field picture of the Flory–Huggins model is validated for a sufficiently large n_{F}.

For linear–linear blends, a one-loop correction from the Flory–Huggins model has been theoretically investigated previously [51,52]. Such studies showed that the correction of χN starts from the order of $1/n_{\mathrm{F}}$, which is $\mathscr{O}(N^{-1/2})$ in the case of ideal lin-

Fig. 3 χN plotted against the interaction parameter ε_{AB} is shown a) for symmetric linear–linear blends and b) for symmetric ring–ring blends. In c), $(\chi N)^{(L,R)}$ values for the ring–ring blends and the linear–linear blends are compared for the same condition of ε_{AB} and N.
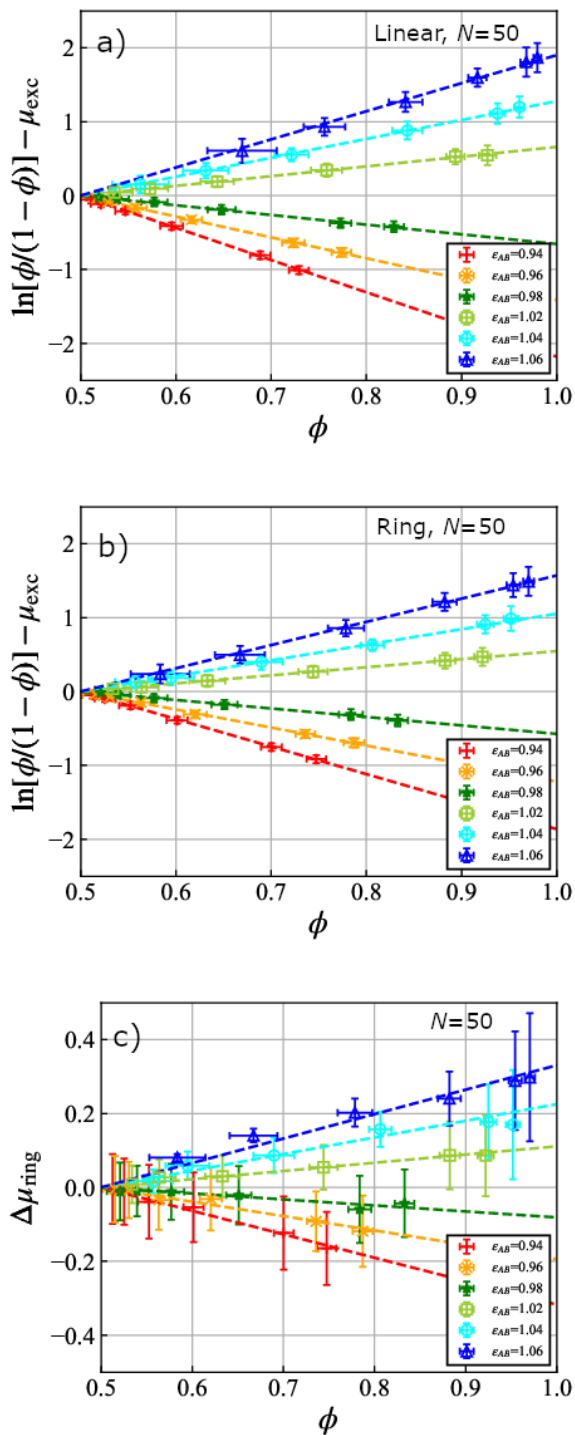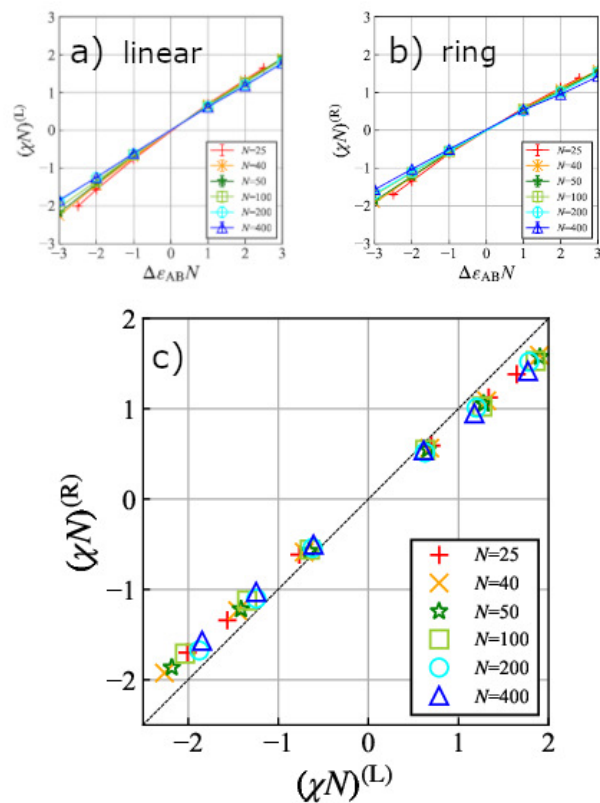

Fig. 2 Results of the SGMC/MD simulations of $N = 50$ a) for linear–linear blends and b) for ring–ring blends. The lines are drawn based on Eq. 3, where χN is determined by fitting. In c), $\Delta\mu_{exc} = \mu_{exc}^{(R)} - \mu_{exc}^{(L)}$ is plotted against ϕ obtained in the $N = 50$ case.

ear chains. A molecular weight dependence and a complex $\Delta\varepsilon_{AB}$ dependence have also been studied by the simulation results of several polymer models [53]. Other calibration models used for extracting χN values are investigated for the systems of finite N and $\Delta\varepsilon_{AB}$ [54]. However, a similar theoretical analysis of ring polymers is more challenging, owing to the need for topology conservation, which restricts the number of possible conformations. Here, we simply use n_F for the ring–ring blends as well as for the linear–linear blends obtained in their single component melts, that is, in the systems where $\varepsilon_{AB} = \varepsilon_0$.

To evaluate the dependence of n_F on χN numerically, we assumed a relationship represented as

$$\frac{(\chi N)^{(L,R)}}{\Delta\varepsilon_{AB}N} = c_0^{(L,R)} + c_1^{(L,R)}\Delta\varepsilon_{AB}N, \quad (5)$$

$$c_0^{(L,R)} = c_{00}^{(L,R)}\left(1 + \frac{c_{01}^{(L,R)}}{n_F}\right), \quad (6)$$

$$c_1^{(L,R)} = \frac{c_{11}^{(L,R)}}{n_F}, \quad (7)$$

where $(\chi N)^{(L,R)}/(\Delta\varepsilon_{AB}N)$ was assumed to linearly depend on $\Delta\varepsilon_{AB}N$. This assumption was supported by the approximate linearity of $(\chi N)^{(L,R)}/\Delta\varepsilon_{AB}N$ on $\Delta\varepsilon_{AB}N$ as shown in Fig. 4. In the previous study [57] on the symmetric linear–linear blends, it was assumed that $c_1^{(L)}$ was almost zero because the observed dependence was very small. However, by extending the data points to the negative region of $\Delta\varepsilon_{AB}N$ and smaller N cases, the $c_1^{(L)}$ dependence becomes more apparent. As we used n_F determined by the case where $\varepsilon_{AB} = \varepsilon_0$, the effect of the interaction difference $\Delta\varepsilon_{AB}$ on the gyration radius was included in the $c_1^{(L,R)}$ term.

It should be noted that the validity of Eq. 5 is restricted in the mixed states and limited within a finite range of $\Delta\varepsilon_{AB}N$. The $c_1^{(L,R)}$ term in Eq. 5 is introduced as an ad-hoc assumption to fit the simulation results. For instance, although Eq. 5 apparently indicates that χN scales $N^{3-3\nu}$, which is $N^{3/2}$ even in linear–linear blends, in the infinitely large limit of N with a fixed value of $\Delta\varepsilon_{AB}$, this cannot be valid for positive $\Delta\varepsilon_{AB}$ in the condition since the systems may undergo phase separation. Also in the case of negative $\Delta\varepsilon_{AB}$, the scaling of $N^{3-3\nu}$ would not be expected. By restricting the application of Eq. 5 within a certain range such that $|\Delta\varepsilon_{AB}N| \leq X$ where X is a constant and independent of N, we obtain $|(\chi N)^{(L,R)}/(\Delta\varepsilon_{AB}N) - c_0^{(L,R)}| \leq c_1^{(L,R)}X$. In fact, our simulation data were limited up to $X = 2.5$ for $N = 25$ systems and $X = 3$ for other systems. The right-hand side, $c_1^{(L,R)}X$, goes to zero from Eq. 7 when $N \to \infty$ for linear–linear blends, and is expected to converge to a constant value for ring–ring blends. It is, however, noted that in our simulations N was limited less than 400 and the exponent $\nu \approx 1/3$ was not observed for ring polymers. Thus, we have adopted Eq. 5 as a simple assumption which at least well captures the simulation results as shown in Fig. 4. Theoretical arguments for the correction term proportional to $\Delta\varepsilon_{AB}N$ are left for future studies.

The prefactor $c_{01}^{(L,R)}$ represents to what extent the interchain interaction varies with the molecular weight. The positive sign
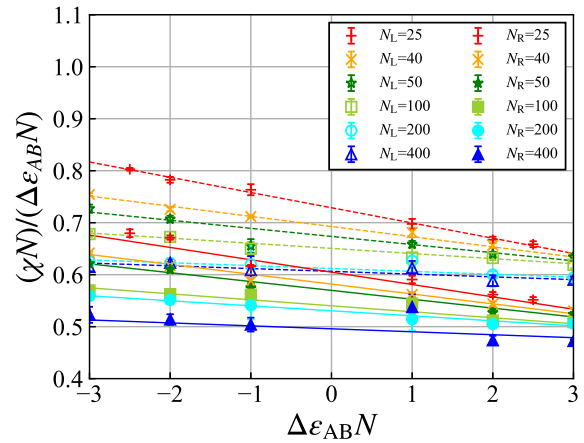

Fig. 4 Value of $(\chi N)^{(L,R)}$ divided by $\Delta\varepsilon_{AB}N$ is shown with respect to $\Delta\varepsilon_{AB}N$. N_L represents the number of beads of linear polymers, and N_R represents the number of beads in ring polymers. The dashed and solid lines are the results of linear regression for the linear–linear blends and the ring–ring blends, respectively.

indicates that the interaction probability of a bead with other beads of different chains increases when the molecular weight decreases. The increase is asymptotically scaled as $\mathcal{O}(1/n_F)$, and the prefactor $c_{01}^{(L)}$ can be derived based on Gaussian chain statistics [52]. $c_{01}^{(L)}$ was predicted as $(1/\pi)^{3/2} \approx 0.180$ for symmetric linear–linear blends [51,52]. Here, we considered $R_g^2 = R_{ee}^2/6$ for linear polymers, and R_{ee}^2 is the squared end-to-end distance.

Figs. 5 a) and b) show the results for $c_0^{(L,R)}$ and $c_1^{(L,R)}$ with respect to $1/n_F$, as obtained by fitting the simulation data of Fig. 3 to Eq. 5. These results confirmed that $c_1^{(L,R)}$ was approximately 10 times smaller than $c_0^{(L,R)}$ in both systems. Thus, the ring topology mostly manifests in the difference of the parameter $c_0^{(R)}$ with respect to $c_0^{(L)}$. For symmetric linear–linear blends, the gradient and intercept of the linear relationship are again consistent with those reported in the previous study [57]. The coefficient $c_{01}^{(L)} \approx 0.14$ for the linear polymers is comparable to the theoretical prediction 0.18. For symmetric ring–ring blends, we obtained $c_{01}^{(R)} \approx 0.074$. The values of $c_{00}^{(L,R)}$ were estimated by extrapolating the simulation data: approximately 0.57 in the linear–linear blends and 0.46 in the ring–ring blends. $c_{11}^{(L,R)}$ were estimated as -0.013 and -0.005, respectively.

In ring polymers, the chains are more compact and the probability of the interchain interaction is lower. The result $c_{01}^{(R)} < c_{01}^{(L)}$ indicates that the molecular weight dependence on the statistical weight of the inter-molecular interaction is smaller than that of the linear chains. In the next section, we evaluate the interaction energy between the beads of the two polymers from the interchain radial distribution functions and compare them with the values of $c_0^{(L,R)}$. It is noteworthy that extrapolation in the infinite limit of n_F for the ring polymers may not be valid because the chain configurations and the Flory exponent of the ring polymers vary in systems with the larger molecular weights. Therefore, the intercepts for ring polymers may also deviate within larger molec-
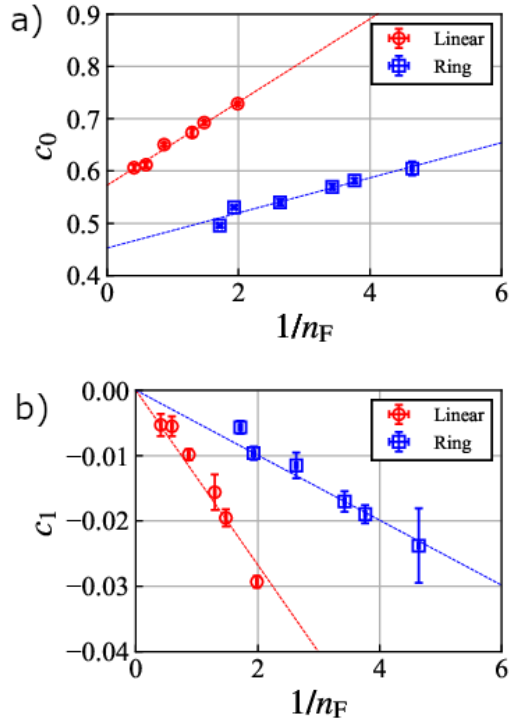
Fig. 5 In a), Coefficient c_0 in Eq. 5 evaluated by fitting the equation to the results of the SGMC/MD simulations. In b), Coefficient c_1 in Eq. 5 is plotted against $1/n_F$. The dashed lines serve as a visual guide.
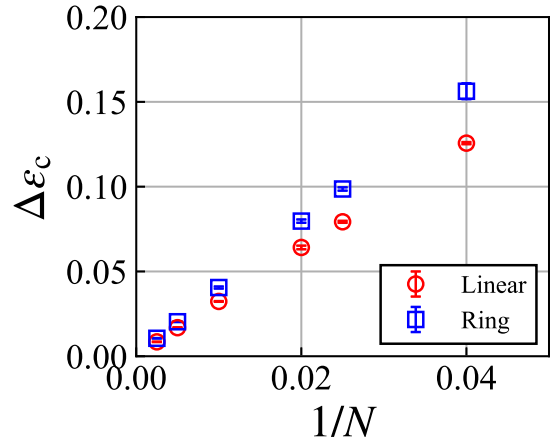

Fig. 6 Critical interaction difference, $\Delta \varepsilon_c$, estimated from the condition that $(\chi N)^{(L,R)} = 2$ is plotted with respect to $1/N$.

ular weight limits.

The effect of ring topology on miscibility was characterized by replacing the parameter $(\chi N)^{(L)}$ with $(\chi N)^{(R)}$; thus, the phase diagram of ϕ versus $\Delta \varepsilon_{AB}$ can be obtained by the phase boundary on the axis of $\Delta \varepsilon_{AB}$ shifting to larger values in the ring–ring blends than in the linear–linear blends. As the critical point, the critical interaction difference, $\Delta \varepsilon_c$, could be estimated by equating $(\chi N)^{(L,R)} = 2$, as shown in Fig. 6 against $1/N$. The critical interaction difference is approximately 25% larger for ring–ring blends compared with those of the corresponding linear–linear blends.

4   Discussion

4.1   Screening effect by topological constraint

To verify the topological effects on miscibility obtained by the SGMC/MD simulations, we compared them with the radial distribution functions of the ring and linear polymers. Because the coefficient $c_1^{(L,R)}$ is much smaller than the coefficient $c_0^{(L,R)}$, the primary effect on χN can be represented by $c_0^{(L,R)}$. As reported in the literature [9,12], the topological constraint may provide a repulsive interaction in the potential of mean force between the ring polymers. This repulsive interaction affects the interchain radial distribution functions, thus the probability of finding a bead of other ring polymers around a bead of a ring polymer is smaller than that in the corresponding linear–linear blends. By using the inter-molecular radial distribution function, χN can be approximated as the first perturbation of $\Delta \varepsilon_{AB}$ from the homopolymer

state as [56]

$$(\chi N)_{rdf} \approx \rho \int d^3 r g_{inter}(r) \left[V_{AB} - \frac{V_{AA} + V_{BB}}{2} \right] N$$

$$= \Delta \varepsilon_{AB} N W \tag{8}$$

where

$$W = 16\pi\rho \int_0^{r_{cut}} dr r^2 g_{inter}(r) \left[\left(\frac{\sigma}{r} \right)^{12} - \left(\frac{\sigma}{r} \right)^6 + \frac{1}{4} \right]. \tag{9}$$

and $g_{inter}(r)$ is the inter-molecular radial distribution function normalized as $g_{inter}(r \to \infty) = 1$. Here, the form of the WCA interaction is considered in obtaining Eq. 9. The coefficient $c_0^{(L,R)}$ in Eq. 5 is approximated by the integral W. The inter-molecular radial distribution functions of the linear chains and ring polymers are shown in Figs. 7 a) and b), respectively. Since the cutoff of the WCA potential is $r_{cut} = 2^{1/6}\sigma$, the shape around the first peak determines the value of the integral W.

We evaluated W for the blends of different molecular weights and the resulting relationship is shown in Fig. 7 c) highlights the consistency between $c_0^{(L,R)}$ and W, supporting the validity of the SGMC/MD simulation results. The result also implies that the interaction energy contribution of ε_{AB} is diminished because the repulsive interaction of the ring topology reduces the probability of inter-molecular interactions between polymers. This reduction may be interpreted as the screening effect of the repulsive interaction on the bare interaction of ε_{AB}. Due to the screening, χN in the ring–ring blends becomes smaller than that of the corresponding linear–linear blends when $\chi N > 0$. Similarly, when $\chi N < 0$, the magnitude of the effective parameter χN is smaller than that of the linear–linear blends.

4.2   Comparison with theoretical and experimental studies

As described in the introduction, Sakaue and Nakajima proposed a model to predict the phase diagram of ring–ring, ring–linear,
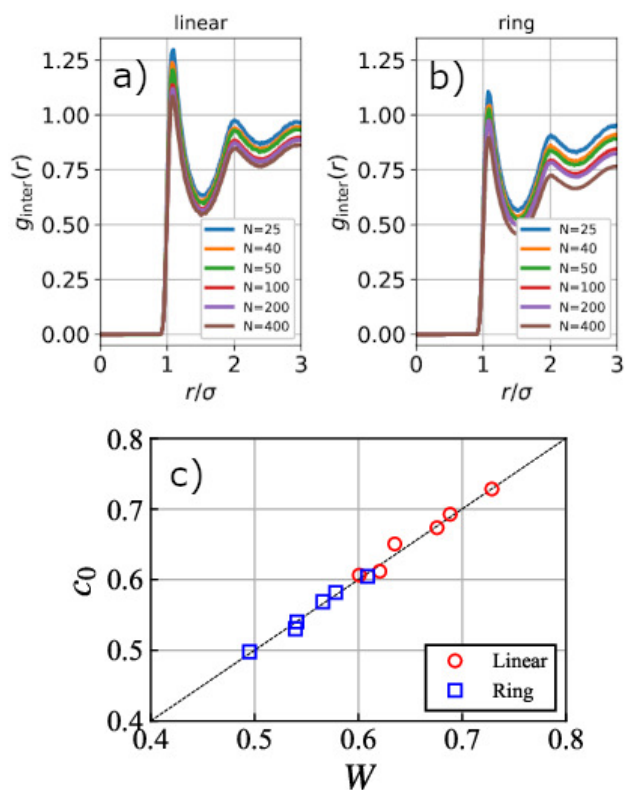
Fig. 7 Inter-molecular radial distribution functions are shown a) for the linear–linear blends and b) for the ring–ring blends. In c), c_0 evaluated by the SGMC/MD simulations is compared to W evaluated from the inter-molecular radial distribution functions in the homopolymer states.

and linear–linear blends using a scaling argument in the limit of large molecular weights [13,44]. To account for the topological effects of ring polymers, they introduced the concept of a *topological volume*. In the symmetric case, $N_A = N_B$, the model predicts that the phase diagram of the ring–ring blends coincides with that of the linear–linear blends (where N_A and N_B represent the number of segments in the polymers of A and B, respectively). However, our simulations in the symmetric blends indicated that the ring–ring blends were slightly more compatible than the linear–linear blends when $\chi N > 0$, contrary to the prediction of the model proposed by Sakaue and Nakajima [13,44].

In their model [13,44], topological effects of ring polymers are accommodated by adding the terms F_{unlink} and F_{unknot} to the standard Flory–Huggins free energy with χ parameter. F_{unlink} represents the entropic penalty from the decrease of free volume due to the topological volume, and F_{unknot} accounts for the unknotting constraint of rings which competes with the shrunk by F_{unlink}. These contributions are vanished in the symmetric systems. As shown in the radial distribution functions in Fig. 7, the coordination number of the interacting bead pairs of different polymers are different even between the symmetric ring–ring blends and the corresponding linear–linear blends. A model of mixing free energy needs to account for this energetic effect resulting from local bead configurations. As mentioned in the introduction, the same conclusion that symmetric ring–ring blends are more compatible has been obtained in the study [48]. It was also pointed out that the miscibility increase for ring–ring blends was attributed to the fewer inter-molecular contacts.

The difference in $c_0^{(L)} - c_0^{(R)}$ remains when the results are extrapolated to a large n_F as shown in Fig. 5 a), implying that χN values at the phase boundary in the ring–ring blends are indeed larger than those of the linear–linear blends; however, as our results are limited to relatively small molecular weights, the extrapolation is not guaranteed to apply to the larger molecular weight limits. Consequently, the extension of this study to larger molecular weights, where the Flory exponent of the gyration radius on N is approximately $1/3$, is needed in the future. Such a simulation would incur high computational costs when equilibrating larger molecular weight systems, Additionally, theoretical arguments for finite molecular weights will also be required in future studies.

In the asymmetric case of $N_A \neq N_B$, the theory predicts that ring–ring blends are less miscible than linear–linear blends. As the SGMC method is not feasible in such asymmetric systems, asymmetric cases were outside the scope of this study and remained as a future study.

There has also been an experimental study on ring topological effects on miscibility [45], in which ring–ring, ring–linear, and linear–linear blends of h-PT and d-PI were prepared. The blend of h-PT and d-PI is known to have lower critical solution temperature (LCST). The results of this experimental study showed that the critical temperature of the ring–ring blend is clearly lower than that of the linear–linear and linear–ring blends, meaning that the ring–ring blends are less miscible than the linear–linear blends. This tendency is consistent with the theoretical prediction when $N_A \neq N_B$. As our simulation model shows phase separation with the upper critical solution temperature (UCST), it is not pos-

sible to determine whether the simulation results can be applied to LCST phase separation, as the mechanism of LCST behavior often depends on the specific conditions of the materials as studied in the preceding study[67]. A model development to describe the LSCT behavior, as has been previously described[68], is therefore necessary to study the topological effects on LCST behavior.

5 Summary

In this study, we investigated the effect of ring topology on miscibility by focusing on the symmetric blends of ring–ring and linear–linear polymers. To evaluate miscibility of ring–ring blends, we investigated the exchange chemical potential as a function of composition and extracted χN numerically as the phenomenological miscibility parameter. Using SGMC and MD simulations, we found that χN for the symmetric ring–ring blends can be evaluated as done for the symmetric linear–linear blends.

By comparing systems in which the molecular weight of the ring and linear polymers were the same, we also found that $(\chi N)^{(R)} \leq (\chi N)^{(L)}$ when $\Delta \varepsilon_{AB} > 0$ and $(\chi N)^{(R)} \geq (\chi N)^{(L)}$ when $\Delta \varepsilon_{AB} < 0$. Hence, the miscible region in the phase diagram of ϕ vs. $\Delta \varepsilon_{AB}$ is larger than that in the linear–linear blends. When $\chi N > 0$, the ring–ring blends are more compatible than linear–linear blends. The origin of this difference is that the bead interaction energy of different chains is smaller in ring–ring blends as verified through the interchain radial distribution functions in the homopolymer melts with several molecular weights. In addition, the dependence of the finite molecular weight on χN was also found to be smaller in ring–ring blends in terms of $1/n_F$ expansions. This implies that the probability of the interchain interactions is less dependent on the chain length in ring–ring blends compared with linear–linear blends.

The systems studied here were limited to symmetric blends and moderately small molecular weights. However, to achieve a fuller understanding, more detailed studies on asymmetric blends and large molecular weight systems are required in the future. The numerical results obtained by computer simulations could help to develop a comprehensive theory for linear–linear, ring–linear and ring–ring blends.

Supplementary Material

Mean squared displacement of the beads against the polymer gyration radius is plotted in Supplementary Material (ESI) for Soft Matter.

Author Contributions

Takahiro Ohkuma: Conceptualization (equal); Data Curation (lead); Formal analysis (equal); Methodology (equal); Investigation (lead); Resources (lead); Visualization (lead); Writing - original draft (lead); Writing - review & editing (equal); **Katsumi Hagita**: Conceptualization (equal); Data Curation (supporting); Formal analysis (equal); Methodology (equal); Resources (supporting); Writing - review & editing (equal); Supervision (lead); **Takahiro Murashima**: Conceptualization (equal); Data Curation (supporting); Formal analysis (equal); Methodology (equal); Resource (supporting); Writing - review & editing (equal); **Tetsuo Deguchi**: Conceptualization (equal); Formal analysis (equal);

Writing - review & editing (equal); Supervision (supporting).

Conflicts of interest

The authors declare that they have no conflicts of interest.

Data Sharing Policy

The data supporting the findings of this study are available from the corresponding author upon reasonable request.

Notes and references

1 T. McLeish, *Science*, 2002, **297**, 2005.

2 C. Micheletti, D. Marenduzzo and E. Orlandini, *Phyics Reports*, 2011, **504**, 1.

3 D. Richter, S. Gooßen and A. Wischnewski, *Soft Matter*, 2015, **11**, 8535.

4 *Topological Polymer Chemistry*, ed. Y. Tezuka and T. Deguchi, Springer Nature Singapore, 2022.

5 V. V. Rybenkov, C. Ullsperger, A. V. Vologodskii and N. R. Cozzarelli, *Science*, 1997, **277**, 690.

6 A. V. Vologodskii, W. Zhang, V. V. Rybenkov, A. A. Podtelezhnikov, D. Subramanian, J. D. Griffith and N. R. Cozzarelli, *Proc. Natl. Acad. Sci. U.S.A.*, 2001, **98**, 3045.

7 G. Witz, G. Dietler and A. Stasiak, *Proc. Natl. Acad. Sci. U.S.A.*, 2011, **101**, 3608.

8 M. D. Frank-Kamenetskii, A. V. Kukashin and A. Vologodskii, *Nature*, 1975, **258**, 398.

9 F. Tanaka, *J. Chem. Phys.*, 1987, **87**, 4201.

10 N. Hirayama, K. Tsurusaki and T. Deguchi, *J. Phys. A: Math. Theor.*, 2009, **42**, 105001.

11 A. Narros, A. J. Moreno and C. N. Likos, *Macromolecules*, 2013, **46**, 3654.

12 A. Narros, C. N. Likos, A. J. Moreno and B. Capone, *Soft Matter*, 2014, **10**, 9601.

13 T. Sakaue, *Reactive and Functional Polymers*, 2019, **134**, 150.

14 F. Guo, K. Li, J. Wu, L. He and L. Zhang, *Polymers*, 2020, **12**, 2659.

15 J. des Cloizeaux, *J. Physique Letters*, 1981, **42**, L433.

16 A. Y. Grosberg, *Phys. Rev. Lett.*, 2000, **85**, 3858.

17 T. Sakaue, *Ring polymers in Melts and Solutions: Scaling and Crossover*, 2011.

18 E. Uehara and T. Deguchi, *J. Chem. Phys.*, 2017, **147**, 214901.

19 M. E. Cates and J. M. Deutsch, *J. Physique*, 1986, **47**, 2121.

20 J. Suzuki, A. Takano, T. Deguchi and T. Matsushita, *J. Chem. Phys.*, 2009, **131**, 144902.

21 T. Vettorel, A. Y. Grosberg and K. Kremer, *Phys. Biol.*, 2009, **6**, 025013.

22 J. D. Halverson, W. B. Lee, G. S. Grest, A. Y. Grosberg and K. Kremer, *J. Chem. Phys.*, 2011, **134**, 204904.

23 J. D. Halverson, G. S. Grest, A. Y. Grosberg and K. Kremer, *Phys. Rev. Lett.*, 2012, **108**, 038301.

24 A. Rosa and R. Everaers, *Phys. Rev. Lett.*, 2004, **112**, 118302.

25 G. B. McKenna, G. Hadziioannou, P. Lutz, G. Hild, C. Strazielle, C. Straupe, P. Rempp and A. J. Kovacs, *Macromolecules*, 1987, **20**, 498.

26 M. Kapnistos, M. Lang, D. Vlassopoulos, W. Pyckhout-Hintzen, D. Richter, D. Cho, T. Chang and M. Rubinstein, *Nature Materials*, 2008, **7**, 997.

27 S. T. Milner and J. D. Newhall, *Phys. Rev. Lett.*, 2010, **105**, 208302.

28 Q. Huang, J. Ahn, D. Parisi, T. Chang, O. Hassager, S. Panyukov, M. Rubinstein and D. Vlassopoulos, *Phys. Rev. Lett.*, 2019, **122**, 208001.

29 D. Parisi, J. Ahn, T. CHang, D. Vlassopoulos and M. Rubinstein, *Macromolecules*, 2020, **53**, 1685.

30 A. Borger, W. Wang, T. C. O'Connor, T. Ge, G. S. Grest, G. V. Jensen, J. Ahn, T. Chang, O. Hassager, K. Mortensen, D. Vlassopoulos and Q. Huang, *ACS Macro Lett.*, 2020, **9**, 1452.

31 J. Wang, T. C. O'Connor, G. S. Grest and T. Ge, *Phys. Rev. Lett.*, 2022, **128**, 237801.

32 T. Murashima, K. Hagita and T. Kawakatsu, *Macromolecules*, 2021, **54**, 7210.

33 D. G. Tsalikis, V. G. Mavrantzas and D. Vlassopoulos, *ACS Macro Lett.*, 2016, **5**, 755.

34 J. Smrek, K. Kremer and A. Rosa, *ACS Macro Lett.*, 2019, **8**, 155.

35 G. D. Papadopoulos, D. G. Tsalikis and V. G. Mavrantzas, *Polymers*, 2016, **8**, 283.

36 T. C. O'Connor, T. Ge, M. Rubinstein and G. S. Grest, *Phys. Rev. Lett.*, 2020, **124**, 027801.

37 K. Hagita, T. Murashima and H. Jinnai, *Polymer*, 2022, **243**, 124637.

38 K. Hagita, T. Murashima, T. Ohkuma and H. Jinnai, *Macromolecules*, 2022, **55**, 6547.

39 A. R. Khokhlov and S. K. Nechaev, *J. Phys. II France*, 1996, **6**, 1547.

40 J. F. Marko, *Macromolecules*, 1993, **26**, 1442.

41 M. Benmouna, S. Khaldi and U. Maschke, *Macromolecules*, 1997, **30**, 1168.

42 M. Müller, *Macromol. Theory Simul.*, 1999, **8**, 343.

43 A. Weyersberg and T. A. Vilgis, *Phys. Rev. E*, 1994, **49**, 3097.

44 T. Sakaue and C. H. Nakajima, *Phys. Rev. E*, 2016, **93**, 042502.

45 Y. Kobayashi, Y. Doi, S. S. A. Rahman, E. Kim, T.-H. Kim, A. Takano and Y. Matsushita, *Macromolecules*, 2018, **51**, 1885.

46 J. U. Kim, Y.-B. Yang and W. B. Lee, *Macromolecules*, 2012, **45**, 3263.

47 Y. Qiang and W. Li, *Macromolecules*, 2021, **54**, 9071.

48 G. S. Grest, T. Ge, S. J. Plimpton, M. Rubinstein and T. C. O'Connor, *ACS Polymers Au*, 2022, https://doi.org/10.1021/acspolymersau.2c00050.

49 P. G. de Gennes, *Scaling concepts in Polymer Physics*, Cornell University Press, 1979.

50 M. Rubinstein and R. H. Colby, *Polymer Physics*, Oxford Univ Press, 2003.

51 J. Qin and D. C. Morse, *J. Chem. Phys*, 2009, **130**, 224902.

52 D. C. Morse and J. K. Chung, *J. Chem. Phys*, 2009, **130**, 224901.

53 J. Glaser, J. Qin, P. Medapuram and D. C. Morse, *Macromolecules*, 2014, **47**, 851.

54 J. D. Willis, T. M. Beardsley and M. W. Matsen, *Macromolecules*, 2020, **53**, 9973.

55 K. Kremer and G. S. Grest, *J. Chem. Phys.*, 1990, **92**, 5057.

56 G. S. Grest, M.-D. Lacasse, K. Kremer and A. M. Gupta, *J. Chem. Phys.*, 1996, **105**, 10583.

57 T. Ohkuma, K. Kremer and K. Daoulas, *J. Phys.: Cond. Matt.*, 2018, **30**, 174001.

58 L. A. Moreira, G. Zhang, F. Müller, T. Stuehn and K. Kremer, *Macromol. Theory Simul.*, 2015, **24**, 419.

59 S. Plimpton, *J. Comput. Phys.*, 1995, **117**, 1.

60 A. Sariban and K. Binder, *J. Chem. Phys.*, 1987, **86**, 5859.

61 A. Sariban, K. Binder and D. W. Heermann, *Phys. Rev. B*, 1987, **35**, 6873.

62 J. D. Halverson, T. Brandes, O. Lenz, A. Arnold, S. Bevc, V. Starchenko, K. Kremer, T. Stuehn and D. Reith, *Comput. Phys. Commun.*, 2013, **184**, 1129.

63 H. V. Guzman, N. Tretyakov, H. Kobayashi, A. C. Fogarty, K. Kreis, J. Krajniak, C. Junghans, K. Kremer and T. Stuehn, *Comput. Phys. Commun.*, 2019, **238**, 66.

64 J. Bicerano, *Prediction of polymer properties*, Marcel Dekker, Inc., 2002.

65 J. D. Londono, A. H. Narten, G. D. Wignall, K. G. Honnell, E. T. Hsieh, T. W. Johnson and F. S. Bates, *Macromolecules*, 1994, **27**, 2864.

66 A. Onuki, *Phase Transision Dynamics*, Cambridge university press, 2002.

67 S. Sakurai, H. Jinnai, H. Hasegawa, T. Hashimoto and C. C. Han, *Macromolecules*, 1991, **24**, 4839.

68 M. Toda, S. Kajimoto, S. Toyouchi, T. Kawakatsu, Y. Akama, M. Kotani and H. Fukumura, *Phys. Rev. E*, 2016, **94**, 052601.